Journal of Advances in Computer Research
Quarterly pISSN: 2345-606x eISSN: 2345-6078
Sari Branch, Islamic Azad University, Sari, I.R.Iran
(Vol. 9, No. 3, August 2018), Pages: 1-21
www.jacr.iausari.ac.ir

# A New Model for Analysis of Unusual Mal-Operation of Differential Protection Due to the Ultra-Saturation Phenomenon during the Loaded Power Transformer Energization

**Bahram Noshad**✉
*Department of Electrical Engineering, Bandar Deylam Branch, Islamic Azad University, Bandar Deylam, Iran*
bahramnoshad@yahoo.com

**Received: 2017/11/05; Accepted: 2018/01/02**

**Abstract**

*In this paper, a new model based on the thevenin equivalent circuit for investigating the ultra-saturation phenomenon during the energization of a loaded power transformer is presented and its effect on the differential protection of the transformer is considered. The ultra-saturation phenomenon causes the mal-operation of the power transformer differential protection. So, the description and control of the ultra-saturation phenomenon is necessary for preventing of the false trip of the differential protection. In this paper, to model the ultra-saturation phenomenon, the nonlinear characteristic of the transformer core, the effect of current transformer, and the core losses are taken into account. It is assumed that the load of the transformer is a resistive and inductive load. Also, the effect of the residual flux and inception angle on the ultra-saturation phenomenon are investigated. The results show that the ultra-saturation phenomenon poses a great problem for protective relaying of power transformers. The outcomes of this research can further be used as hints for substation operation personnel as well as for the development of new protection stabilization criteria, which is not discussed further in this paper. The explanation of the ultra-saturation phenomena is the first step toward developing new ideas and criteria for more reliable transformer protection that would better handle such abnormal cases than currently employed relaying equipment. In this paper, the fourth-order Runge-Kutta method is used to solve the equations and simulation of the ultra-saturation phenomenon is done by MATLAB program.*

***Keywords:*** *Loaded Transformer Energization, Transformer Differential Protection, Ultra-Saturation Phenomenon, Mal-Operation*



## 1. Introduction

The power transformer protection is an important component in power systems. The effect of magnetizing inrush currents has to take into account in power transformer protective scheme. This is because the magnetizing inrush current, which occurs when a transformer is energized on the transmission line or an external line fault is cleared, sometimes results in 10 times full load currents and hence can cause mal-operation of the differential relays. The differential protective system establishes the main protection against short circuit faults on primary and secondary windings of transformer. This

protective system should operate rapidly during internal faults. However, it should not operate under non-internal fault conditions such as inrush current. The most common technique used to prevent false trips during the energization of power transformer is harmonic restraint relays. The principle of the harmonic restraint relays is based on that the second harmonic and sometimes the fifth harmonic component of the inrush current is considerably larger than in a typical fault current [1,2]. Normally, in order to discriminate between the internal fault and inrush current, an algorithm is used in which the differential protection operates when the magnitude of the fundamental component of differential current stabilizes above 0.25p.u and the ratio of the second harmonic to fundamental harmonic of the differential current stabilizes below 15% [3-7]. But it has been reported that in certain conditions the mal-operation of differential protection under inrush current has caused tripping of healthy transformers [5-7]. In [5-7], the mal-operation of differential protection during the energization of the loaded transformer was reported whose origin is known as ultra-saturation phenomenon. The authors observed that energization of a loaded transformer may cause the situation, called ultra-saturation, when the DC flux in the core in the initial stage of the process increases rather than decreasing [5]. Hence, the distortion of the current wave shape gets smaller, and the percentage of the second harmonic decreases below the relay restraining level [5-7]. In this case, the current ac wave shape is approximately undistorted and the level of the second harmonic is negligible. For the analytical study of the ultra-saturation phenomenon, a preliminary loaded transformer energization model is suggested [5]. Using this model, the delayed mal-operation of differential protection can be described [8-10]. In [5], many simplifications during the simulations are carried out which take the magnetizing reactance of the time-variant characteristic as an equivalent inductance, neglecting the core model of the transformer, without considering the transferring effect of current transformer to the primary inrush, and consider only the resistive load, can be mentioned which does not coincide with the real situation. Hanli Weng, Xiangning Lin and Pei Liu revised their previous model in 2007. According to them the previous theory cannot be utilized directly to analyze this phenomenon. Therefore, a new model for analyzing the transient behavior of the loaded transformer energization, together with the current transformer model involving the magnetic hysteresis effect, taking the nonlinear magnetizing reactance, and no considering only the resistive load is proposed [6]. But in [6], the core losses of the transformer are neglected and a difficult model for current transformer in primary side is considered whose main difficulty in current transformer modeling is the simulation of the hysteresis loop. Andrzej Wiszniewski et al. the conditions which must be met to make ultra-saturation and excessive ultra-saturation possible are presented in 2008 [7]. The ATP-EMTP program is used for simulation. In [7], the core model of the transformer and the magnetizing reactance are neglected and this does not coincide with the real situation.

In this paper, a new model based on the thevenin equivalent circuit for investigating the ultra-saturation phenomenon during the energization of a loaded power transformer is presented and its effect on the differential protection of the transformer is considered. In this model, the nonlinear characteristic of the transformer core, the effect of current transformer, and the core losses are taken into account. It is assumed that the load of the transformer is a resistive and inductive load. In addition to a new model for power transformer, the effective model for current transformer is presented in this paper. The main advantages of this proposed model in compare with previous models are as following:

1) The core losses are taken into account.

2) A new model has been considered for current transformers. In this model, information of B-H curve for magnetic branch isn't required. Also, since hysteresis effect isn't taken into account, result can be compared with the IEEE model considering hysteresis effect.

3) It involves proper computing speed and accuracy.

4) Also, the mal-operation of the differential protection depends on a variety of factors the most important parameters of which are residual flux and inception angle. In this paper the parameters mentioned will be studied in various scenarios. The explanation of the ultra-saturation phenomena is the first step toward developing new ideas and criteria for more reliable transformer protection that would better handle such abnormal cases than currently employed relaying equipment. In this paper, the fourth-order Runge-Kutta method is used to solve equations and simulation of the ultra-saturation phenomenon is done by MATLAB.

The paper is organized as follows. Section 2 introduces the modeling of the loaded power transformer to study the ultra-saturation phenomenon. Section 3 presents a new model for current transformer. The proposed algorithm is presented in section 4. Simulation of the ultra-saturation phenomenon is presented in section 5. Finally, Conclusions and future work are given in section 6.

## 2. Modeling of the Loaded Power Transformer

The loaded transformer energization can be described by the equivalent circuit as illustrated in Figure 1.

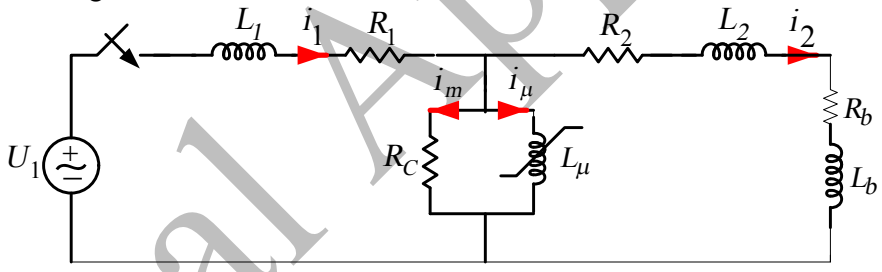


***Figure 1. Circuit of the loaded transformer energization***

In this model, $U_1$ is the electromotive force of the source, $L_1$ and $R_1$ represent the inductive and the resistive components of the equivalent impedance comprising of system impedance and leakage impedance of transformer primary winding. $L_2$ and $R_2$ represent the inductive and resistive components of the equivalent impedance comprising of the leakage impedance of transformer secondary winding and the impedance of burden. The magnetizing nonlinear branch of transformer core is illustrated by an equivalent inductance $L_\mu$. For determining the new model, according to Figure 2, the nonlinear magnetizing branch of transformer is removed and the thevenin equivalent circuit is obtained from points A and B.

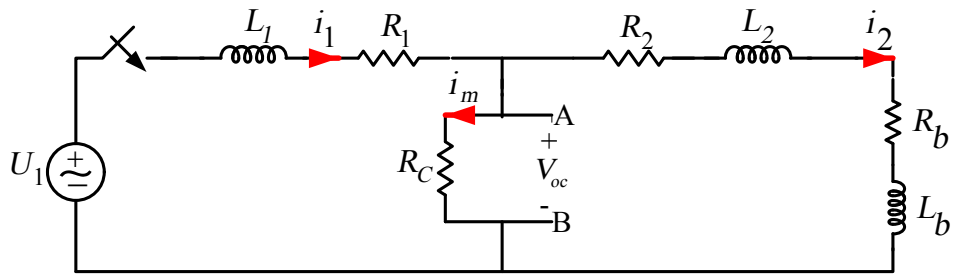


***Figure 2. Equivalent circuit model for determination the thevenin voltage and impedance***

The power supply is defined as:

$$U_1(t) = U_m \sin(\omega t + \theta) \tag{1}$$

According to equivalent circuit in Figure 2, the thevenin voltage is:

$$V_{oc} = (A_1 + A_2)\cos\omega t + \frac{(B_1 + B_2)}{\omega}\sin\omega t + (C_1 + C_2)e^{-bt}\cos\sqrt{a}t + \frac{(D_1 - C_1 b + D_2 - C_2 b)}{\sqrt{a}}e^{-bt}\sin\sqrt{a}t \tag{2}$$

Where $A_1 = \dfrac{(a_2 - \omega^2 - \frac{R_2}{L_2}a_1)a_3}{(a_2 - \omega^2)^2 + a_1^{\,2}\omega^2}$, $A_2 = \dfrac{(\omega^2 a_1 + \frac{R_2}{L_2}(a_2 - \omega^2))a_4}{(a_2 - \omega^2)^2 + a_1^{\,2}\omega^2}$,

$B_1 = \dfrac{a_3 - (a_2 - \omega^2)A_1}{a_1}$, $B_2 = \dfrac{\frac{R_2}{L_2}a_4 - (a_2 - \omega^2)A_2}{a_1}$, $C_1 = -A_1$, $C_2 = -A_2$,

$D_1 = -A_1 a_1 - B_1$, $D_2 = a_4 - A_2 a_1 - B_2$,

$a = \dfrac{R_1 R_2}{L_1 L_2} + \dfrac{R_1 R_C}{L_1 L_2} + \dfrac{R_2 R_C}{L_1 L_2} - \dfrac{1}{4}(\dfrac{R_1}{L_1} + \dfrac{R_2}{L_2} + \dfrac{R_C}{L_2} + \dfrac{R_C}{L_1})^2$, $b = \dfrac{1}{2}(\dfrac{R_1}{L_1} + \dfrac{R_2}{L_2} + \dfrac{R_C}{L_2} + \dfrac{R_C}{L_1})$,

$a_1 = \dfrac{R_C L_2 + R_C L_1 + R_2 L_1 + R_1 L_2}{L_1 L_2}$, $a_2 = \dfrac{R_2 R_C + R_1 R_C + R_1 R_2}{L_1 L_2}$, $a_3 = \dfrac{R_C U_m \omega \cos\theta}{L_1}$,

$a_4 = \dfrac{R_C U_m \sin\theta}{L_1}$.

And also, the thevenin impedance is:

$$Z_{th} = (R_1 + jX_1)\|(R + jX_2)\|(R_C) = R_{th} + jX_{th} \tag{3}$$

Where $R_{th} = \dfrac{A_1^{\,2}R_C + A_1 R_C^{\,2} + B_1^{\,2}R_C}{(A_1 + R_C)^2 + B_1^{\,2}}$, $X_{th} = \dfrac{B_1 R_C^{\,2}}{(A_1 + R_C) + B_1^{\,2}}$,

$A_1 = \dfrac{R_1^2 R + R_1 R^2 + R_1 X_2^2 + R\,X_1^2}{Z^2}$, $B_1 = \dfrac{X_1^2 X_2 + X_1 X_2^2 + R_1^2 X_2 + X_1 R^2}{Z^2}$,

$Z = \sqrt{(X_1 + X_2)^2 + (R_1 + R\,)^2}$, $L_{th} = \dfrac{X_{th}}{\omega}$, $X_1 = L_1\omega$, $X_2 = L\omega$.

Due to (3), the thevenin impedance is an equivalent resistance and inductance. After obtaining the thevenin model of the nonlinear magnetizing branch from points A and B, the nonlinear magnetization branch is returned to the circuit as shown in Figure 3.

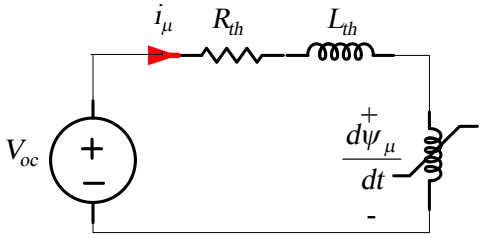


***Figure 3. Simplified circuit model of loaded power transformer***

According to Figure 3, the nonlinear magnetizing branch current $i_\mu$ is a function of $\psi_\mu$. The accurate curve of $\psi_\mu - i_\mu$ should be shown as a multi-valued curve if taking the hysteresis into account. For the convenience of solving the equations, the magnetization curve can be simplified, as shown in Figure 2. It can be assumed that the saturation point is $(i_{\mu 0}, \psi_S)$. The inductance in saturation region and no saturation region are $L_s$ and $L_\mu$, respectively. It should be emphasized that the inductance of the magnetizing branch of transformer is still nonlinear, even if the above simplification is used. Hence, according to Figure 2 $i_\mu$ can be defined as follow:

$$i_\mu = \begin{cases} \dfrac{\psi_\mu - \psi_s}{L_s} + i_{\mu_0} & \psi_\mu > \psi_s \\ \dfrac{\psi_\mu + \psi_s}{L_s} - i_{\mu_0} & \psi_\mu < -\psi_s \\ i_{\mu_0} \dfrac{\psi_\mu}{\psi_s} & |\psi_\mu| \le \psi_s \end{cases} \tag{4}$$

Where $\psi_\mu$ is the flux linkages, $\psi_S$ is the flux linkages at the knee point of the magnetization curve, $i_{\mu 0}$ is the magnetization current at the knee point of the magnetization curve and $L_s$ is the slope of the saturation curve.

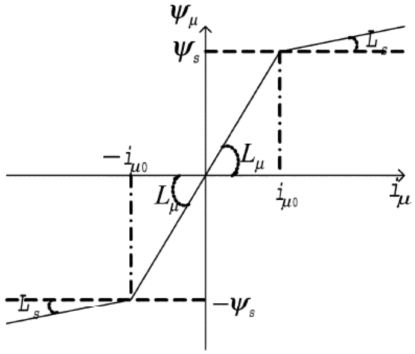


***Figure 4. The approximate magnetizing characteristic of transformer core***

The magnetization curve shown in Figure 4 is divided into three regions.

Region 1: $\psi_\mu > \psi_s$

In this case the magnetization current is defined:

$$i_\mu = \frac{(\psi_\mu - \psi_s)}{L_s} + i_{\mu_0} \tag{5}$$

According to equivalent circuit in Figure 3:

$$-V_{oc} + R_{th} i_\mu + L_{th} \frac{di_\mu}{dt} + \frac{d\psi_\mu}{dt} = 0 \tag{6}$$

Substitute (5) into (6):

$$-V_{oc} + R_{th}\left(\frac{\psi_\mu - \psi_s}{L_s} + i_{\mu_0}\right) + \left(\frac{L_{th}}{L_s}\right)\frac{d\psi_\mu}{dt} + \frac{d\psi_\mu}{dt} = 0 \tag{7}$$

According to (7):

$$\frac{d\psi_\mu}{dt} = \frac{V_{oc}}{1+\frac{L_{th}}{L_s}} - \frac{R_{th}}{1+\frac{L_{th}}{L_s}}\left(\frac{\psi_\mu - \psi_s}{L_s} + i_{\mu_0}\right) \tag{8}$$

Region 2: $\psi_\mu < -\psi_S$

In this case the magnetization current is defined:

$$i_\mu = \frac{1}{L_s}(\psi_\mu + \psi_s) - i_{\mu_0} \tag{9}$$

According to (6) and (9):

$$-V_{oc} + R_{th}\left(\frac{\psi_\mu + \psi_s}{L_s} - i_{\mu_0}\right) + \left(\frac{L_{th}}{L_s}\right)\frac{d\psi_\mu}{dt} + \frac{d\psi_\mu}{dt} = 0 \tag{10}$$

Due to (10):

$$\frac{d\psi_\mu}{dt} = \frac{V_{oc}}{1+\frac{L_{th}}{L_s}} - \frac{R_{th}}{1+\frac{L_{th}}{L_s}}\left(\frac{\psi_\mu + \psi_s}{L_s} - i_{\mu_0}\right) \tag{11}$$

Region 3: $|\psi_\mu| \le \psi_s$

In this case the magnetization current is defined:

$$i_\mu = i_{\mu_0}\frac{\psi_\mu}{\psi_s} \tag{12}$$

According to (6) and (12):

$$-V_{oc}+R_{th}(\psi_\mu\frac{i_{\mu_0}}{\psi_s})+L_{th}(\frac{i_{\mu_0}}{\psi_s})\frac{d\psi_\mu}{dt}+\frac{d\psi_\mu}{dt}=0 \quad (13)$$

Due to (13):

$$\frac{d\psi_\mu}{dt}=\frac{V_{oc}}{1+\frac{L_{th}i_{\mu_0}}{\psi_s}}-\frac{R_{th}}{1+\frac{L_{th}i_{\mu_0}}{\psi_s}}(\psi_\mu\frac{i_{\mu_0}}{\psi_s}) \quad (14)$$

According to equivalent shown in Figure 1:

$$\frac{d\psi_1}{dt}+R_1i_1+\frac{d\psi_\mu}{dt}=U_1 \quad (15)$$

$$i_1=i_2+i_\mu+i_m \quad (16)$$

$$\frac{d\psi_\mu}{dt}=\frac{d\psi_2}{dt}+R_2i_2 \quad (17)$$

Where $i_m=\frac{1}{R_C}\frac{d\psi_\mu}{dt}$. Due to (15) and $i_1=\psi_1/L_1$:

$$\frac{d\psi_1}{dt}=U_1-R_1(\frac{\psi_1}{L_1})-\frac{d\psi_\mu}{dt} \quad (18)$$

## 3. Current Transformer Modeling

The equivalent circuit of a current transformer is shown in Figure 5. In this circuit $R_1$ and $L_1$ are the resistive and the inductive components of the equivalent impedance comprising of system impedance and leakage impedance of transformer primary winding. $R_2$ and $L_2$ are resistance and inductance of the secondary side of the current transformer. $R_b$ and $L_b$ are resistance and inductance burden. Since the core loss doesn't affect the behavior of the current transformer saturation, it is neglected [11]. The equivalent circuit of the current transformer, referred to the secondary side, is shown in Figure 6.

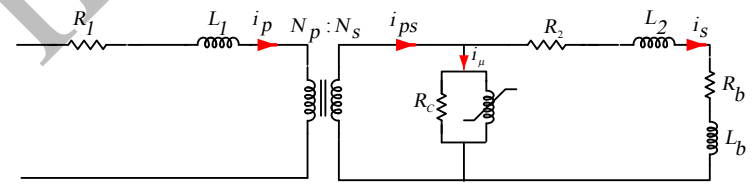


***Figure 5. Equivalent circuit of current transformer***

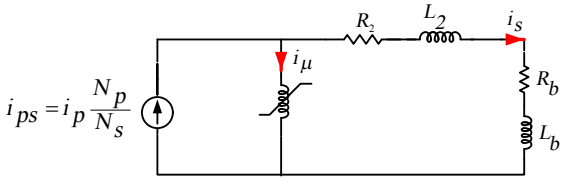


***Figure 6. Equivalent circuit of current transformer referred to secondary side***

The magnetization curve illustrated in Figure 4 is used for current transformer core that $\psi_s$ and $i_{\mu_0}$ are different for power transformer and current transformer. To model the current transformer, equivalent circuit shown in Figure 6 is considered. In this circuit, we defined:

$$\begin{aligned} R &= R_2 + R_b \\ L &= L_2 + L_b \end{aligned} \tag{19}$$

According to the equivalent circuit shown in Figure 6:

$$i_{ps} = i_\mu + i_s \tag{20}$$

$$e_s = Ri_s + L\frac{di_s}{dt} \tag{21}$$

$$i_{ps} = \frac{N_p}{N_s} i_p \tag{22}$$

In these equations, $i_{ps}$ is the primary current referred to secondary side, $i_\mu$ is the magnetizing current, $i_s$ is the secondary current, $N_p$ is the number of primary turns, $N_s$ is the number of secondary turns, and $e_s$ is the induced voltage in the secondary winding. According to (20):

$$i_s = i_{ps} - i_\mu \tag{23}$$

According to Figure 4, the magnetization curve is divided into three regions.

Region 1: $\psi_\mu > \psi_s$

$$i_\mu = \frac{(\psi_\mu - \psi_s)}{L_s} + i_{\mu_0} \tag{24}$$

According to (23) and (24):

$$i_s = i_{ps} - \frac{1}{L_s}(\psi_\mu - \psi_s) - i_{\mu_0} \tag{25}$$

Differentiate from (25):

$$\frac{di_s}{dt} = \frac{di_{ps}}{dt} - \frac{1}{L_s}\frac{d\psi_\mu}{dt} \tag{26}$$

Due to $\frac{d\psi_\mu}{dt} = e_s$ from (21), (25) and (26):

$$\frac{d\psi_\mu}{dt} = \frac{RL_s}{L_s + L}\left(i_{ps} - \frac{(\psi_\mu - \psi_s)}{L_s} - i_{\mu_0}\right) + \frac{LL_s}{L_s + L}\left(\frac{di_{ps}}{dt}\right) \tag{27}$$

Region 2: $\psi_\mu < -\psi_s$

$$i_{\mu} = \frac{1}{L_s}(\psi_{\mu} + \psi_s) - i_{\mu_0} \tag{28}$$

According to (23) and (28):

$$i_s = i_{ps} - \frac{1}{L_s}(\psi_{\mu} + \psi_s) + i_{\mu_0} \tag{29}$$

Differentiate from (29):

$$\frac{di_s}{dt} = \frac{di_{ps}}{dt} - \frac{1}{L_s}\frac{d\psi_{\mu}}{dt} \tag{30}$$

Due to $\frac{d\psi_{\mu}}{dt} = e_s$ from (21), (29) and (30):

$$\frac{d\psi_{\mu}}{dt} = \frac{RL_s}{L_s + L}(i_{ps} - \frac{(\psi_{\mu} + \psi_s)}{L_s} + i_{\mu_0}) + \frac{LL_s}{L_s + L}(\frac{di_{ps}}{dt}) \tag{31}$$

Region 3: $|\psi_{\mu}| \le \psi_s$

$$i_{\mu} = i_{\mu_0}\frac{\psi_{\mu}}{\psi_s} \tag{32}$$

According to (23) and (32):

$$i_s = i_{ps} - i_{\mu_0}\frac{\psi_{\mu}}{\psi_s} \tag{33}$$

Differentiate from (33):

$$\frac{di_s}{dt} = \frac{di_{ps}}{dt} - \frac{i_{\mu_0}}{\psi_s}\frac{d\psi_{\mu}}{dt} \tag{34}$$

Due to $\frac{d\psi_{\mu}}{dt} = e_s$ from (21), (33) and (34):

$$\frac{d\psi_{\mu}}{dt} = \frac{R\psi_s}{\psi_s + i_{\mu_0}}(\frac{N_p}{N_s}i_{ps} - i_{\mu_0}\frac{\psi_{\mu}}{\psi_s}) + \frac{L\psi_s}{\psi_s + i_{\mu_0}}(\frac{N_p}{N_s}\frac{di_{ps}}{dt}) \tag{35}$$

## 4. Proposed Algorithm

The differential protection should be able to distinguish the internal faults from the external faults, the magnetizing inrush current and the ultra-saturation phenomenon and it should only operate under internal faults. Normally, in order to distinguish between the external faults, internal faults and magnetizing inrush current, an algorithm is used in which the differential protection operates when the amplitude of the basic component of the differential current fixes upper than 0.25 p.u and the level of the second harmonic to basic harmonic of the differential current fixes lower than 15%. But it has been described that in certain conditions the false trip of differential protection under

magnetizing inrush current has led to tripping of healthy transformers. One of transient phenomenon that leads to the false trip of the power transformer differential protection during the energization of a loaded power transformer is the ultra-saturation phenomenon. In this paper, a new model based on the thevenin equivalent circuit for investigating the ultra-saturation phenomenon during the energization of a loaded power transformer is presented. To model the ultra-saturation phenomenon, first the differential currents of phases are obtained from subtraction of secondary currents of current transformers on the primary and secondary side of the power transformers. Then, the following steps are performed:

a) The steady state amplitudes of the basic component of the differential currents ($i_{dss}$) are calculated by the use of the Discrete Fourier Transform (DFT) algorithm. If the steady state amplitude fixes lower than 0.25 p.u., the normal condition will be occurred. Otherwise, the ultra-saturation phenomenon may be occurred and must calculate the second harmonic to the basic harmonic.

b) The ratio of the second harmonic to the basic harmonic ($\frac{H_2}{H_{base}}$) of the differential currents is calculated by the use of the DFT algorithm. If the ratio fixes lower than 15%, the mal-operation of the power transformer differential protection due to the ultra-saturation is occurred.

So, according to above steps, if the differential protection uses 0.25 p.u. as the operating threshold for the amplitude of the basic component of differential currents and 15% as the second harmonic restraint ratio, the false trip occurs due to the ultra-saturation. The flowchart of proposed algorithm is shown in Figure 7.

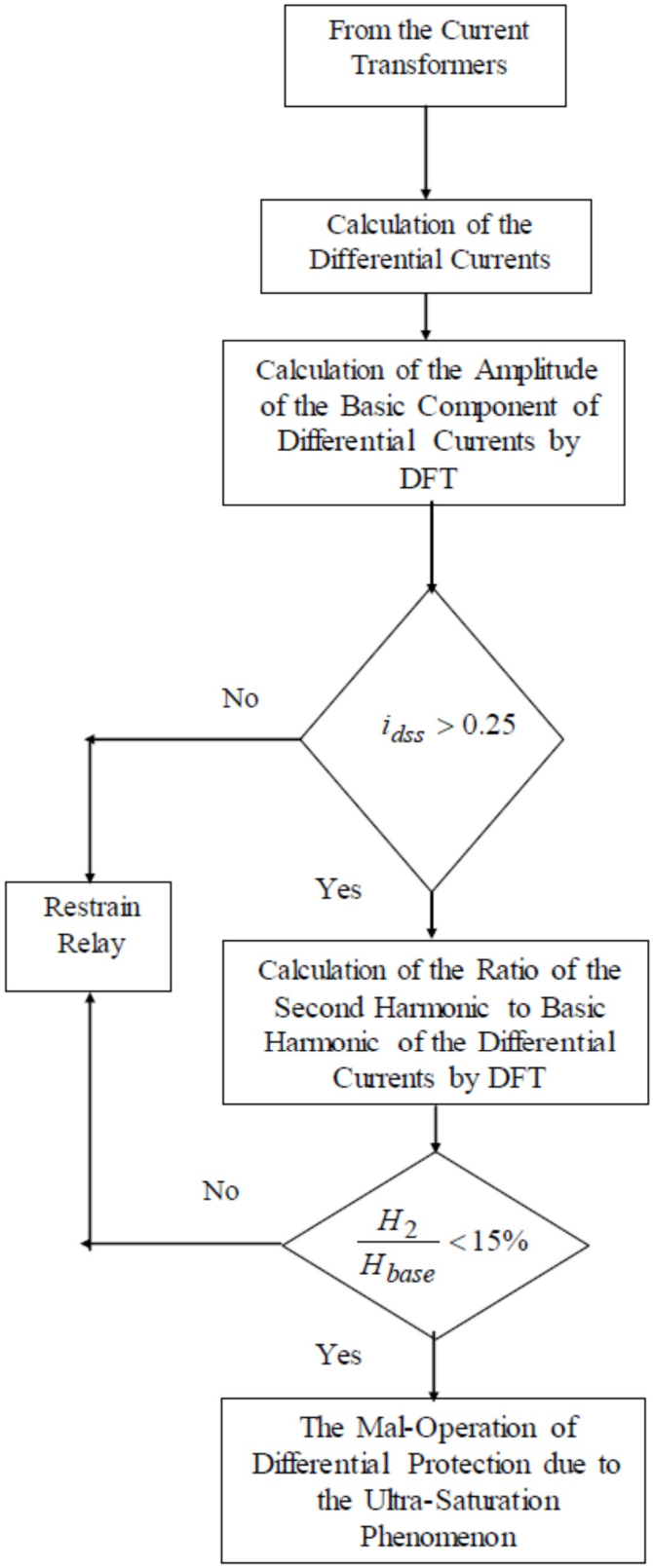


***Figure 7. Flowchart of the proposed algorithm***

## 5. Simulation of the Ultra-Saturation Phenomenon

It is supposed that the transformer has load connected and is energized from the high-voltage side at $t = 0$. The source parameters are:

$U_1(t) = U_m \sin(\omega t + \theta)$

$U_m = 110 \ \ kV$

$\omega = 100\pi \ \ rad$

$\theta = 0^\circ$

Where $\theta$ is the phase angle of phase A when the transformer is connected to the voltage source. The transformer parameters are:

$k = 110/35 \ \ kV$

$L_1 = 0.06 \ \ H, \ \ R_1 = 15 \ \ \Omega$

$L_2 = 0.035 \ \ H, \ \ R_2 = 115 \ \ \Omega$

$R_C = 13.7 \ \ k\Omega$

$\psi_m = U_m/\omega$

$\psi_s/\psi_m = 1.2$

$L_\mu = 500H, \ \ L_s = 0.01H, \ \ i_{\mu 0} = \psi_s / L_\mu$

Parameters for the current transformer on the high-voltage side of the power transformer are:

$k = 600/5, \ \ B_s = 1.8T, \ \ L_s = 0.7mH, \ \ A = 3.472e^{-3}m^2, \ \ \psi_s = 0.75wb*turns,$

$i_{\mu 0} = 0.05mA, \ \ R = 0.05\Omega$

Parameters for the current transformer on the low-voltage side of the power transformer are:

$k = 2400/5, \ \ B_s = 1.9T, \ \ L_s = 0.7mH, \ \ A = 3.53e^{-3}m^2, \ \ \psi_s = 1.34wb*turns,$

$i_{\mu 0} = 0.03mA, \ \ R = 0.15\Omega$

$\psi_\mu$ and $\psi_1$ can be solved from (8), (11), (14), and (18) by using the forth-order Runge-Kutta method with a 10μs time step. The Figure 8 shows the curve of the magnetic linkage in the core after transformer energization. The magnetic current $i_\mu$ according to (4), the primary current according to $i_1 = \psi_1 / L_1$ and the secondary current according to (16) have been calculated using the computed $\psi_\mu$ and $\psi_1$ that are shown in Figures 9, 10, and 11, respectively.

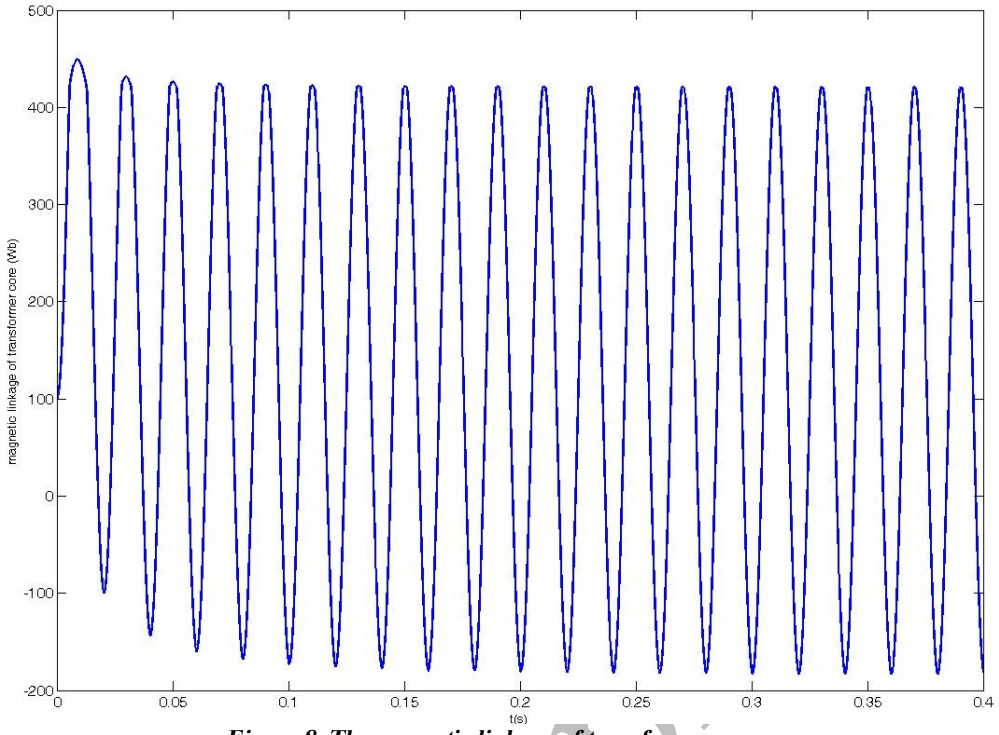


***Figure 8. The magnetic linkage of transformer core***

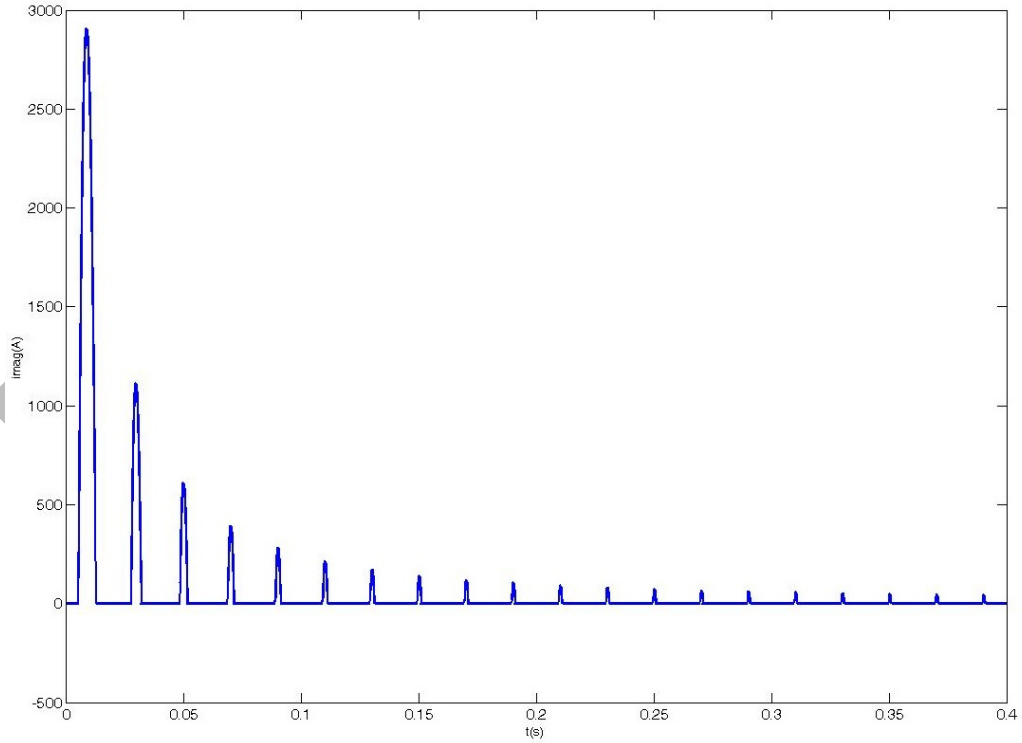


***Figure 9. The current of transformer magnetizing branch***

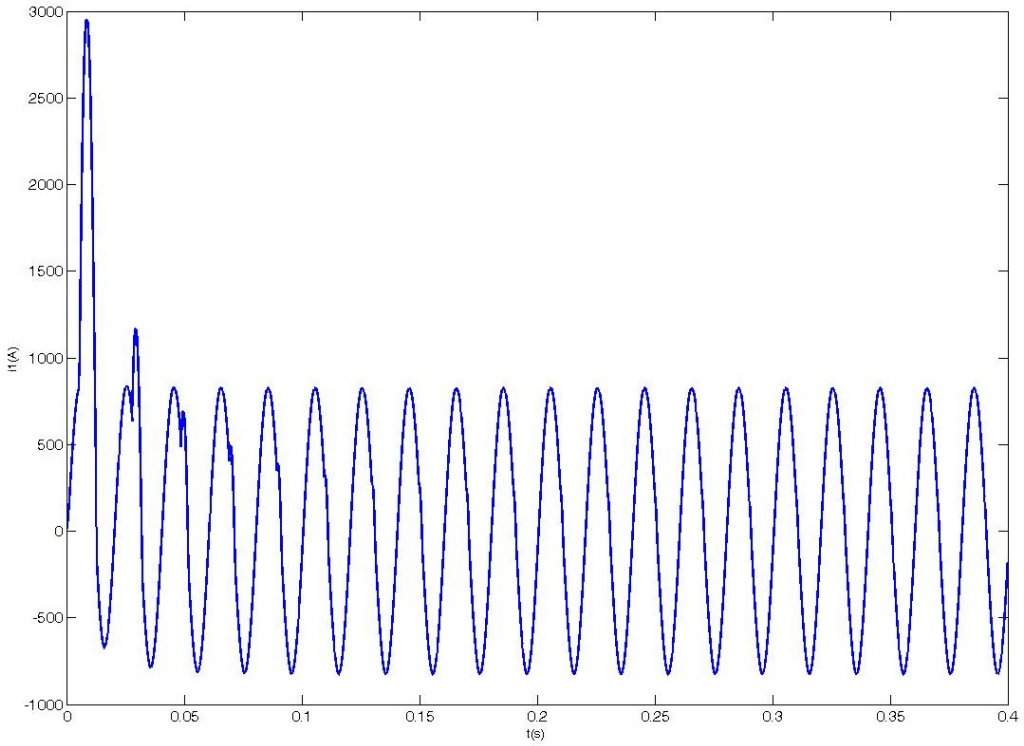


***Figure 10. The primary current of the transformer***

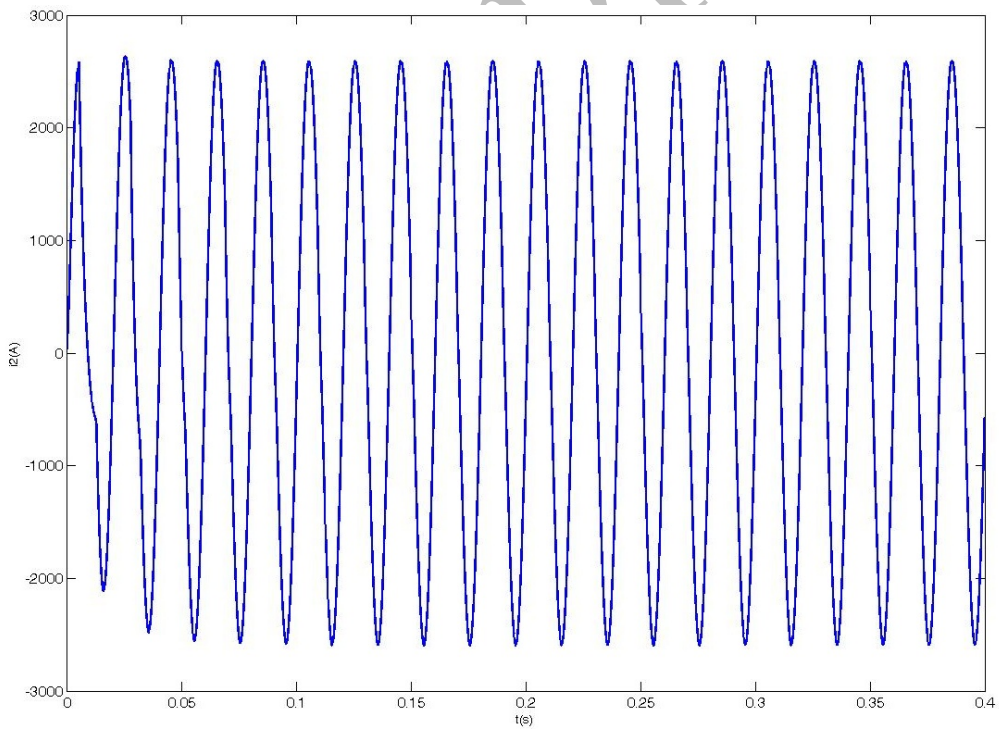


***Figure 11. The secondary current of the transformer***

$i_1$ is the primary current of current transformer on the primary side of power transformer and $i_2$ is the primary current of current transformer on the secondary side of power transformer. Now the secondary currents of current transformers on primary and secondary side of power transformer should be achieved. $\psi_\mu$ is related to current transformers on the primary and secondary side of power transformer and can be solved from (27), (31) and (35) using any numerical integration method. In this analysis, the forth-order Runge-Kutta method has been used with a 10μs time step. The magnetic current $i_\mu$ according to (4) and the secondary current of current transformers according to given (25), (29) and (33) are calculated using the computed$\psi_\mu$. In these relations, $i_{ps}$ is the primary current of power transformer. In Figure 12, the primary current refers to secondary side and secondary current of the current transformer on the primary side of the transformer are shown, that are $i_{11}$ and $i_{12}$ respectively. In Figure 13, the primary current refers to the secondary side and secondary current of the current transformer on the secondary side of the transformer are shown, that are $i_{21}$ and $i_{22}$ respectively. Also the differential current ($i_d$) shown in Figure 14 can be obtained from subtract $i_{12}$ and $i_{22}$.

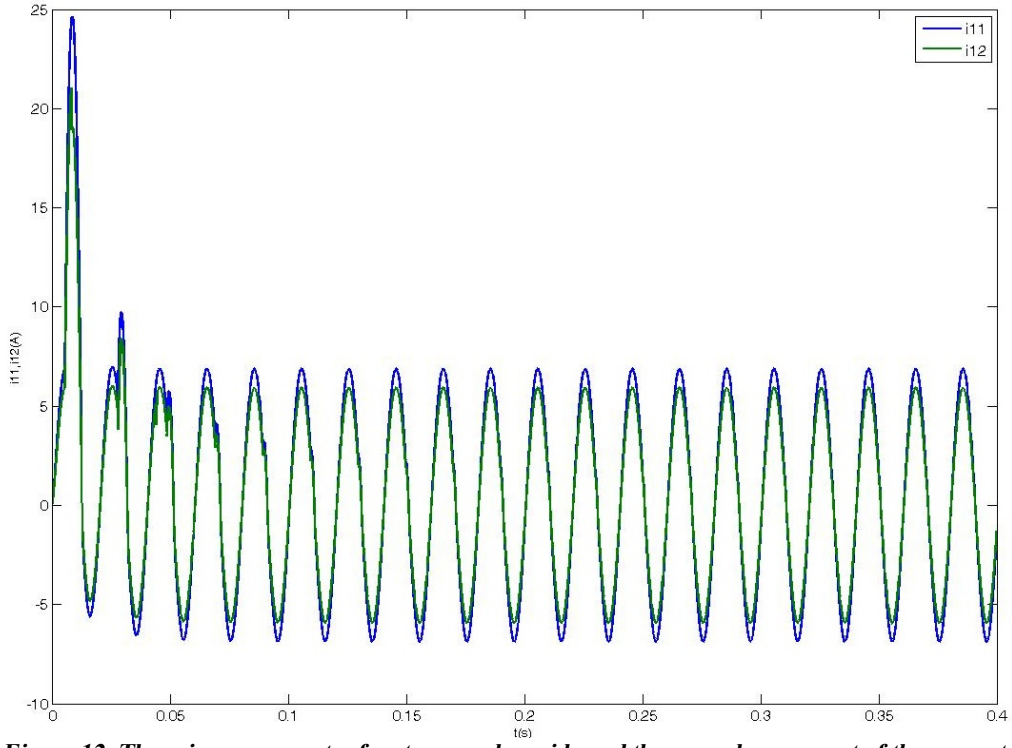


***Figure 12. The primary current refers to secondary side and the secondary current of the current transformer on the primary side of the power transformer***

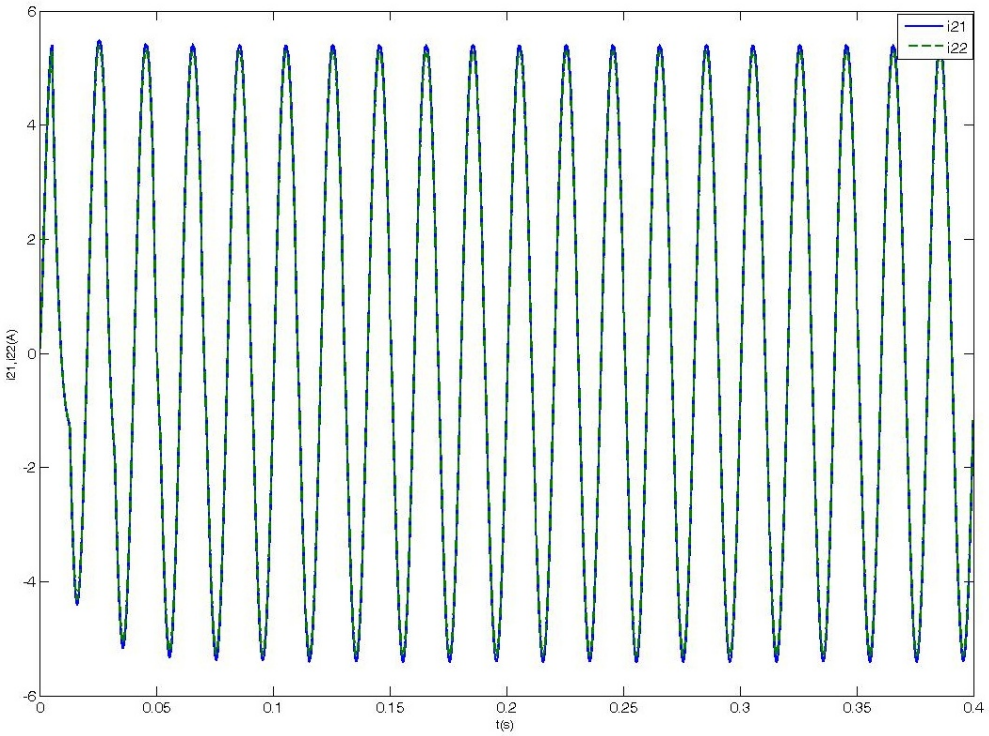


***Figure 13. The primary current refers to secondary side and the secondary current of the current transformer on the secondary side of the power transformer***

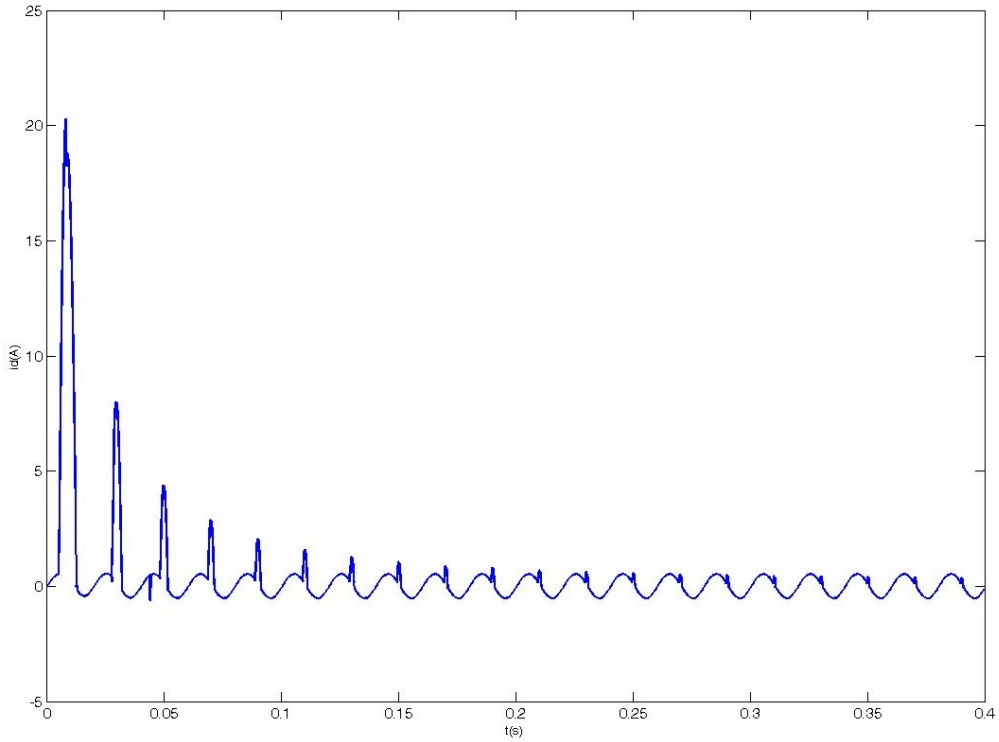


***Figure 14. Waveform of the differential current***

As illustrated in Figures. 12 and 13, the primary current of the power transformer contains much higher aperiodic component because of the nonlinearity of the transformer core, but the aperiodic component on the secondary current of the power transformer is very low. In this case, the current transformers of both sides in the transforming behavior differ so greatly that the false differential current (Figure 14) with significant amplitude and relatively low harmonic contents will likely be formed because of the transforming difference of the current transformers. Figure 15 displays the changes of the magnitude of the fundamental component of $\dot{I}_d$ in Figure 14, which is obtained with the Discrete Fourier Transform (DFT) algorithm. In this Figure the magnitude of the fundamental component of the differential current is normalized according to the secondary current of current transformers.

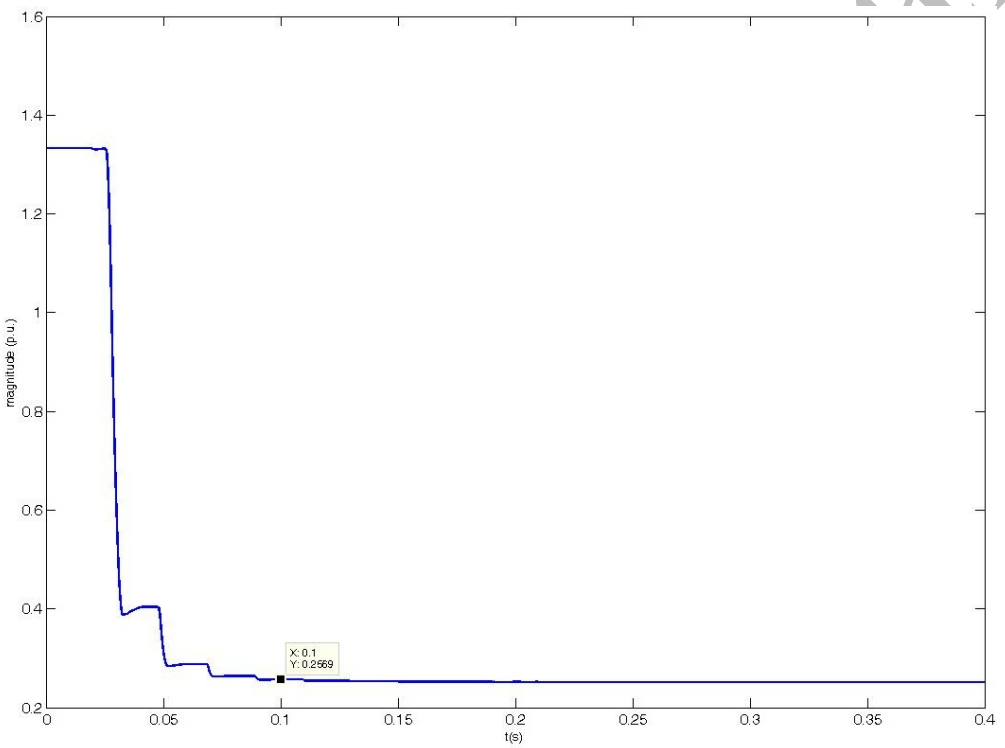


***Figure 15. The normalized magnitude of the fundamental component of the differential current***

Figure 16 displays the ratio change of the second harmonic to fundamental harmonic of the differential current after energization which is obtained with the DFT algorithm.

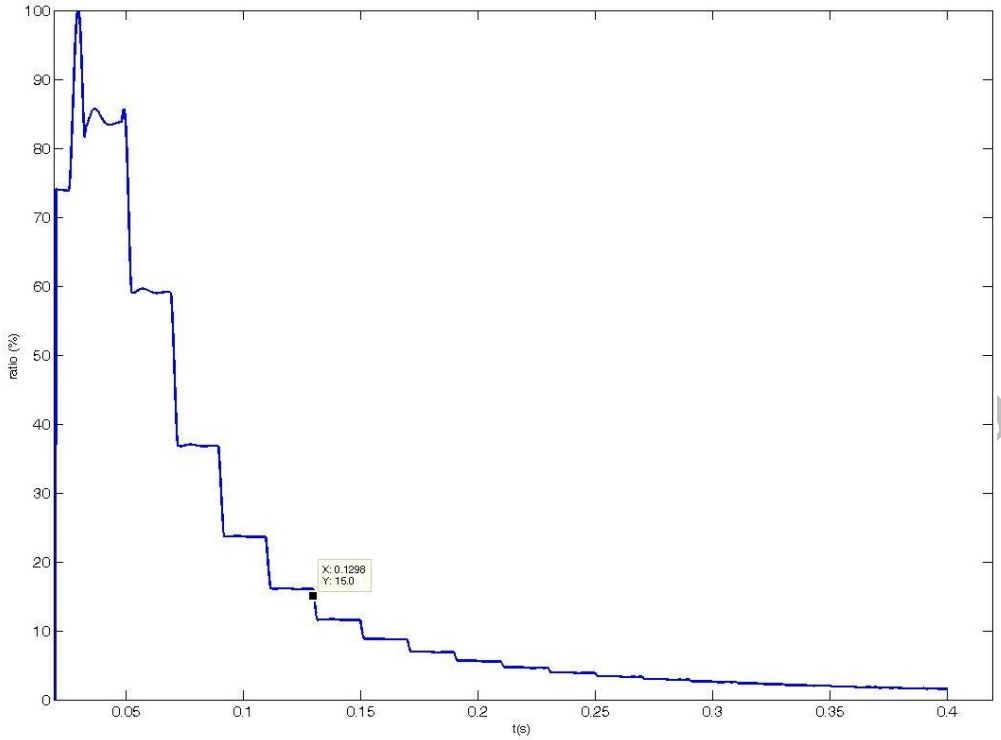


***Figure 16. Ratio of second harmonic to fundamental harmonic of the differential current with DFT algorithm***

As illustrated in Figure 15, the fundamental component of differential current is above 0.25p.u from the beginning of energization and approximately, after 5 cycles (0.1s) it is stabilised on 0.2569p.u. According to Figure 16, as the energization time exceeds 0.1298s, the ratio of the second harmonic to fundamental harmonic stabilizes below 15%. If the differential protection uses 0.25 p.u. as the operating threshold and 15% as the second harmonic restraint ratio, the mal-operation occurs at 0.1298s. The occurrence of the delayed mal-operation of the differential protection depends on a variety of factors that the most important which can be noted residual flux and inception angle. In the previous simulations the inception angle was 0 degrees and the residual flux was 100 Webbers as shown in Figure 8. In tables 1 and 2, various scenarios for different inception angles and residual fluxes are presented, respectively.

***Table 1. Various scenarios for different inception angles***

| $\theta$ $(^\circ)$ | $\psi_\mu(0)$ $(wb)$ | $m$ $(p.u.)$ | $t_a$ $(s)$ | $t_{trip}$ $(s)$ |
|---|---|---|---|---|
| 0 | 100 | 0.2569 | 0.1298 | 0.1298 |
| 20 | 100 | 0.2567 | 0.11 | 0.11 |
| 40 | 100 | 0.2551 | 0.1083 | 0.1083 |
| 60 | 100 | 0.2545 | 0.107 | 0.107 |
| 80 | 100 | 0.2525 | 0.1057 | 0.1057 |

***Table 2. Various scenarios for different residual fluxes***

| $\psi_\mu(0)$ $(wb)$ | $\theta$ $(^\circ)$ | $m$ $(p.u.)$ | $t_a$ $(s)$ | $t_{trip}$ $(s)$ |
|---|---|---|---|---|
| -100 | 0 | 0.2545 | 0.1106 | 0.1106 |
| -50 | 0 | 0.2553 | 0.1109 | 0.1109 |
| 0 | 0 | 0.256 | 0.1112 | 0.1112 |
| 50 | 0 | 0.2566 | 0.1297 | 0.1297 |
| 100 | 0 | 0.2569 | 0.1298 | 0.1298 |

In tables 1 and 2, $m$ ،$t_a$ و $t_{trip}$ are the magnitude of reaching the fundamental component of the differential current to 0.1s, the time of reaching the ratio of second harmonic to fundamental harmonic of the differential current to 15% and the time of the differential protection tripping, respectively. According to table 1, the extreme cases of inrush occur in inception angle of zero and as the inception angle increases, the time of the tripping of the differential protection decreases. As shown in table 2, if residual flux increases, the time of the tripping of the differential protection increases.

## 6. Conclusions and Future Work

In this paper, a new model based on thevenin equivalent circuit for investigating the ultra-saturation phenomenon during the energization of a loaded power transformer was presented and its effect on the differential protection of the transformer was considered. In this model, the nonlinear characteristic of the transformer core, the effect of current transformer, and the core losses were also taken into account. It was assumed that the load of the transformer is a resistive and inductive load. In addition to a new model for power transformer, the effective model for current transformer was presented in this paper. The primary current of the power transformer contains much higher aperiodic component because of the nonlinearity of the transformer core but the aperiodic component on the secondary current of the power transformer is very low. In this case, the current transformers of both sides in the transforming behavior differ so greatly that the false differential current with significant amplitude and relatively low harmonic contents will likely be formed because of the transforming difference of the current transformers which causes the ultra-saturation phenomenon to occur. The mal-operation of the differential protection depended on a variety of factors the most important parameters of which were residual flux and inception angle. Finally, the parameters mentioned were studied in various scenarios. The results showed that the ultra-saturation was a likely phenomenon. The main advantages of this proposed model in compare with previous models were as following:

1) The core losses were taken into account.

2) A new model has been considered for current transformers. In this model, information of B-H curve for magnetic branch wasn't required. Also, since hysteresis effect wasn't taken into account, result could be compared with the IEEE model considering hysteresis effect.

3) It involved proper computing speed and accuracy.

4) Also, the mal-operation of the differential protection depended on a variety of factors the most important parameters of which were residual flux and inception angle.

In this paper the parameters mentioned studied in various scenarios. The explanation of the ultra-saturation phenomena is the first step toward developing new ideas and

criteria for more reliable transformer protection that would better handle such abnormal cases than currently employed relaying equipment. In this paper, the fourth-order Runge-Kutta method was used to solve equations.

This work presented here concentrates on the phenomenon itself, trying to explain when excessive flux without zero crossing may appear. Knowing why and when the ultra-saturation may occur, one may better understand the possible cases of the differential protection mal-operation. The outcomes of this paper may be also treated as hints for substation personnel, defining the system configurations, and parameters that should be avoided in order to be on the safe side should unfavorable energization occur. It seems that improvement of the protection operation would be possible with the introduction of new, modified, or extended criteria. The protection criteria should, on one hand, carry enough information on the event to be distinguished and, on the other hand, ensure appropriate stabilization for other events for which protection operation is undesirable. Certain proposals of such new criteria can be found in the literature, such as a complex second harmonic restraint, flux restraint (estimated on basis of voltages), or current wave shape analysis; others still wait for their inventors. It is believed that a lot of improvement can be reached with the introduction of adaptivity in the differential protection, a simple example of which is to use adaptive thresholds as well as adaptive measurement procedures. It has also been proved that considerable improvement of the operation and quite simple achievement of adaptive features of protection functions may be obtained with the use of various artificial-intelligence techniques. There is hope that an appropriate combination of classical and intelligent techniques should bring additional benefits; therefore, further investigations on the subject are desirable.

## References

[1] P. Liu, O. P. Malik, D. Chen, Hope GS, Guo Y, "Improved operation of differential protection of power transformers for internal faults", IEEE Trans Power Deliver, 1992.

[2] A. Kunakorn, "Application of discrete wavelet transform for transformer inrush current detection in protective control scheme", In: Proceedings of the international symposium on communications and information technologies conference, 2004.

[3] A.Wiszniewski, H. Ungrad, and W.Winkler, "Protection Techniques in Electrical Energy Systems", New York: Marcel Dekker, 1995.

[4] "Numerical Differential Protection Relay for Transformers, Generators, Motors and Mini Bus bars," SIEMENS AG, 7UT613/63x V.4.06 Instruction Manual, Order. C53000-G1176-C160-2, 2006.

[5] X. Lin and P. Liu, "The Ultra-Saturation Phenomenon of Loaded Transformer Energization and Its Impacts on Differential Protection," IEEE Transactions on power delivery, 2005.

[6] H. Weng, X. Lin, and P. Liu, "Studies on the Operation Behavior of Differential Protection during a Loaded Transformer Energization," IEEE Transactions on power delivery, 2007.

[7] A. Wiszniewski, W. Rebizant, D. Bejmert, and L. Schiel, "Ultra saturation Phenomenon in Power Transformers—Myths and Reality," IEEE Transactions on power delivery, 2008.

[8] M. Taghipour, S. M. Razavi, and M. A. Shamsinejad, "Intelligent Determining Amount of Inter-Turn Stator Synchronous Motor Using an Artificial Neural Network Trained by Improved Gravitational Search Algorithm", Journal of Advances in Computer Research, 2014.

[9] M. Taghipour, M. Yazdani, S. A. Gholamian, and M. Razavi, "A Novel Approach for Discrimination Magnetizing Inrush Current and Internal Fault in Power Transformers Based on Neural Network", Journal of Advances in Computer Research, 2014.

[10] S. M. B. Sadati, J. Moshtagh, A. Rastgou, "Load and Harmonic Forecasting for Optimal Transformer Loading and Life Time by Artificial Neural Network", Journal of Advances in Computer Research, 2015.

[11] M. Naidu and G.W. Swift, "Dynamic Analysis of a current Transformer during Faults", Electric Power System Research, 1986.